Reports

Ballistic 2-D Imaging Through Scattering Walls Using an Ultrafast Optical Kerr Gate

L. WANG, P. P. HO, C. LIU, G. ZHANG, R. R. ALFANO

An ultrafast optical shutter was used to image ultrasmall objects hidden behind scattering walls by a procedure that selects in time the ballistic component and rejects the scattered diffusive light. Scattering walls used in this experiment included human breast tissue, chicken breast tissue, and a water suspension of polystyrene particles with scattering coefficients up to 21.7. Submillimeter resolution was achieved for two-dimensional ballistic images of a single point, a double-point fluorescence source, and a bar test chart in or behind these different turbid media.

RECENT REPORTS (*1, 2*) SHOW THAT one in ten women will develop breast cancer, which is the number one killer for women over 40 years old. A significant reduction in this mortality depends on early detection in which a cure rate of over 80% can be achieved (*1*). Unfortunately, x-ray mammography cannot detect tumors at their early stage of development. For earlier diagnosis, it is important to image ultrasmall growths with a size of 1 mm or less. Optical radiation (*3–6*) offers a method to image a small tumor hidden inside the human body. Transillumination, a technique in which light is used to image breast cancer, was introduced several years ago. In this technique (*7–9*), visible light is incident on a breast, and a shadow image of the tumor may be observed on the opposite side of the breast. However, the ability to observe this image is severely limited by light scattering in the breast, which reduces the intensity of the unscattered light that forms the image shadow and contributes to the noise. The reduction of the unscattered light with respect to the scattered light limits transillumination as a viable technique with which to detect breast cancer to a spatial resolution greater than 1 cm. When the tumor is either too small (a few millimeters) or lies deep inside the breast, it may not be observed by the transillumination technique. One needs to modify the technique (*10*) by adding an ultrafast time gate if one hopes to significantly improve the detectability of small tumors located inside the breast.

L. Wang, P. P. Ho, C. Liu, G. Zhang, Department of Electrical Engineering, Institute for Ultrafast Spectroscopy and Lasers, The City College and the Graduate School of The City University of New York, New York, NY 10031.
R. R. Alfano, Departments of Electrical Engineering and Physics, Institute for Ultrafast Spectroscopy and Lasers, The City College and the Graduate School of The City University of New York, New York, NY 10031.

When photons migrate through a turbid medium, there are three main signal components (*4*): (i) diffusive (incoherent) photons, (ii) ballistic (coherent, forward-scattered) photons that arrive first by traveling over the shortest path, and (iii) snake (quasi-coherent) photons that arrive within the first δt after traveling over relatively short paths (Fig. 1A). The diffusive scattered photons of the signal travel over a much larger distance in turbid samples (*11, 12*) than those of ballistic or snake photons, which take shorter paths through the medium within a small forward angular cone. It is believed that the ballistic and snake components contain the least distorted image information and that the diffusive component loses most of the image information. Time-resolved techniques can separate out the ballistic and snake components from the diffusive component of light migration in turbid media.

In this report, using a two-dimensional (2-D) picosecond optical Kerr gate imaging system, we demonstrate ballistic 2-D images that spatially resolved phantom point source 200 μm in diameter and a phantom bar test chart with bars 100 μm wide in highly scattering media including a 3.5-mm-thick sample of human breast tissue, a 3-mm-thick sample of chicken breast tissue, and a 5-cm-thick water cell with suspended polystyrene balls. The experimental setup of the picosecond Kerr gate (*13–15*) imaging system consisted of a mode-locked Nd:glass laser, a CS_2 Kerr shutter, and a 2-D readout system. The laser pulse has a peak power of 5×10^8 W, a duration time of 8 ps, and a wavelength of 1054 nm. The pulse energy is ~4 mJ. The 1054-nm laser beam is sent through a potassium dihydrogen phosphate crystal to produce the second harmonic component with a wavelength of 527 nm and a peak power of about 10^7 W, which is the probing source to illuminate the hidden object. The typical transmission efficiency of a CS_2 Kerr shutter was ~10%. The image was recorded by an intensified 2-D charged-coupled device (CCD) camera with 640 by 480 pixels, a gain of 6000 times, and a dynamic range of 100:1. Its minimum detection level is ~1 lux cm^{-2}. A PC computer, a frame grabber, software package, and video printer were used to store, process, and display the images. All photographs shown in Figs. 2 and 3 were obtained from a single laser shot, which consisted of a laser train with ~100 pulses each separated by ~10 ns.

Hidden objects in various scattering walls, including human breast tissue, chicken breast tissue, and a model system (polystyrene spheres in a water cell) were detected with this system. The picosecond Kerr gate was capable of separating the ballistic image from the diffusive noise. Figure 1B displays the images of ballistic and diffusive components from a point source inside a scattering medium. The scattering medium consisted of polystyrene spheres of diameter ~0.46 μm suspended in water in an optical cell with the dimension 5 by 5 by 5 cm^3. The volume density of the spheres was 0.88% for all measurements except in the double quasi–point source measurement for which the density was 0.3%. The calculated scattering coefficient was $N\sigma L \sim 21.7$ for the single point source and bar chart and $N\sigma L \sim 7.4$ for the double quasi–point source fluorescence imaging test, where N is the number density of scattering particles, σ is the scattering cross section, and L is the thickness of the sample. When a piece of breast tissue is used as a scattering medium, its total attenuation coefficient is $\mu_a + \mu_s$ (~2.5 to 600 cm^{-1}) (*7, 16–18*), where μ_a is the absorption coefficient and μ_s is the scattering coefficient.

To produce a single quasi–point source, a 527-nm laser beam was focused onto a ground glass plate placed inside the scattering medium. The diameter of the focal beam spot was ~200 μm. To produce a double quasi–point source, the 527-nm beam was split into two beams and focused onto a polydiacetylene (PDA) film 200 μm thick placed inside the scattering medium to form a fluorescence double point source. The emission spectrum for PDA is from 550 to 850 nm with a fluorescence lifetime (*19*) of ~12 ps.

The Kerr gate image intensity for a single point source and the bar chart in a scattering medium are plotted in Fig. 1C as a function of delayed gating time. The ballistic signal corresponds to intensity located at a gating time of about $t = 0$. The peak of the diffusive component follows the ballistic signal and appeared at ~20 ps.

The time-gated images of the single 200-μm point source at different gating times are displayed in Fig. 2 as 2-D video photo-

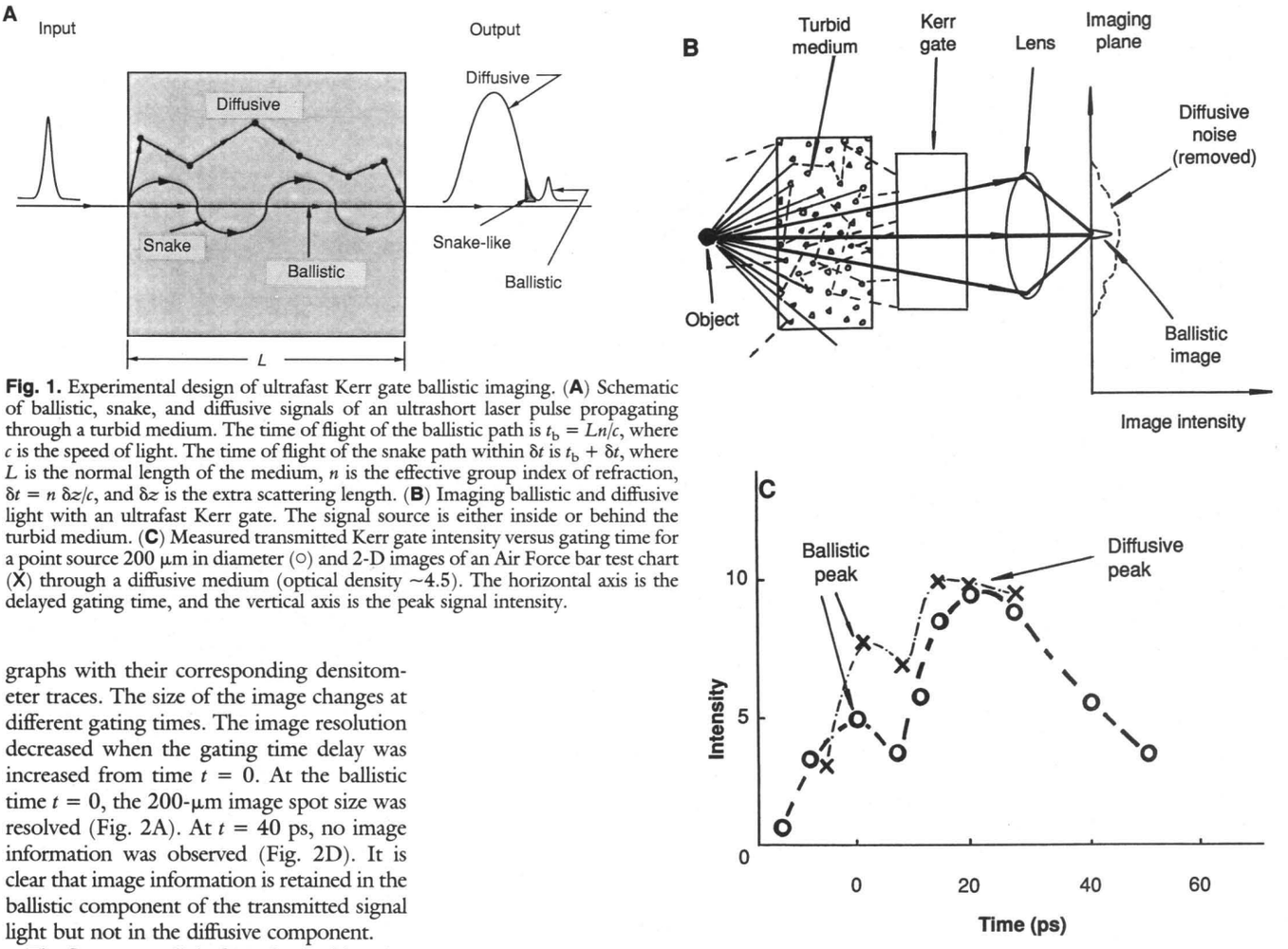

Fig. 1. Experimental design of ultrafast Kerr gate ballistic imaging. (**A**) Schematic of ballistic, snake, and diffusive signals of an ultrashort laser pulse propagating through a turbid medium. The time of flight of the ballistic path is $t_b = Ln/c$, where c is the speed of light. The time of flight of the snake path within δt is $t_b + \delta t$, where L is the normal length of the medium, n is the effective group index of refraction, $\delta t = n\,\delta z/c$, and δz is the extra scattering length. (**B**) Imaging ballistic and diffusive light with an ultrafast Kerr gate. The signal source is either inside or behind the turbid medium. (**C**) Measured transmitted Kerr gate intensity versus gating time for a point source 200 μm in diameter (○) and 2-D images of an Air Force bar test chart (X) through a diffusive medium (optical density ~4.5). The horizontal axis is the delayed gating time, and the vertical axis is the peak signal intensity.

graphs with their corresponding densitometer traces. The size of the image changes at different gating times. The image resolution decreased when the gating time delay was increased from time $t = 0$. At the ballistic time $t = 0$, the 200-μm image spot size was resolved (Fig. 2A). At $t = 40$ ps, no image information was observed (Fig. 2D). It is clear that image information is retained in the ballistic component of the transmitted signal light but not in the diffusive component.

The fluorescence light from the double point source separated by ~400 μm has also been resolved by the picosecond Kerr gate and is not resolved by the steady-state transillumination imaging. For the steady-state image, the double point image merged into strong noise wings. The diameter of each fluorescence point source was ~200 μm. PDA film situated inside turbid water ($N\sigma L = 7.4$) was illuminated by two 527-nm laser pulses. The resolved image of the two point sources separated by 400 μm was formed by the ballistic part of the signal light.

A sequence of measured time-dependent 2-D Kerr-gated video images of a bar chart that was hidden behind 3.5-mm-thick human breast tissue and 3-mm-thick chicken breast tissue are displayed in Fig. 3, A and B, respectively. The bars of the test chart (five line pairs per millimeter ~100-μm spatial resolution) were illuminated by 8-ps, 527-nm laser pulses. Figure 3, A1 and B1, represents the reference photographs, which display the image of the test chart without the scattering wall. Figure 3, A2 and B2, represents the images obtained from standard transillumination imaging (no time gate) of the chart behind these two tissue samples; no clear image can be observed in either of these cases. Figure 3, A3 and B3, shows the Kerr gate bar images of the ballistic and snake signals at a gating time of $t = 0$ (time resolution δt ~10 ps). Clear bar images with dimension of ~0.1 mm (separated by 0.2 mm) can be resolved in human breast tissue in Fig. 3, A3 (*3*). As the gating time was delayed by 22 ps, the collected images were gradually broadened and blurred as shown in Fig. 3, A4 and B4. These results demonstrate that the 2-D Kerr imaging system as opposed to 1-D time-gated imaging systems (*5, 6, 20*) can be used to image phantom in vitro human organs and tissues.

Figure 4 shows the measured image visibility of the bar chart in water with suspended balls ($N\sigma L$~7.4) at different delay times. The image contrast [≡ fringe visibility = $(I_{max} - I_{min})/(I_{max} + I_{min})$, where I is intensity] at $t = 0$ was ~80%, dropping to 3% at $t = 33$ ps.

From the data presented in Figs. 2 and 3 when the gating time was set at $t = 0$, the ballistic component of the transmitted light image was imaged with a resolution of ~200 μm. When the gating time was delayed, the scattering noise background increased with time (Fig. 2, B and C). When the gating time became greater than 0, the ballistic light disappeared and the diffusive scattering light dominated the image quality; a point image could not be measured. For the 2-D bar chart measurements, time-gated ballistic images can be obtained through breast tissues with sub-millimeter resolution. When the gating time was further delayed, images became brighter and the spatial resolution became poorer. The stronger diffusive scattering light blurred the images. One reason that the measured contrast at $t = 0$ was only 80% instead of 100% was that the finite gating time (8-ps laser pulse) allowed some diffusive scattering noise to pass through the gate within the gating time, and this partially blurred the image. Shorter pulses and faster gates can achieve better image contrast ratios.

To improve the spatial resolution and signal-to-noise (S/N) ratio in a thick scattering wall, one needs to use (i) shorter pulses on the order of 100 fs for the time gate where a 100-μm spatial resolution can be achieved through 60-mm-thick breast; (ii) a cooled CCD detector with a multiple pulse signal acquisition and high repetition rate to improve the S/N ratio by a factor of 10^5; and (iii) a multistage cascade

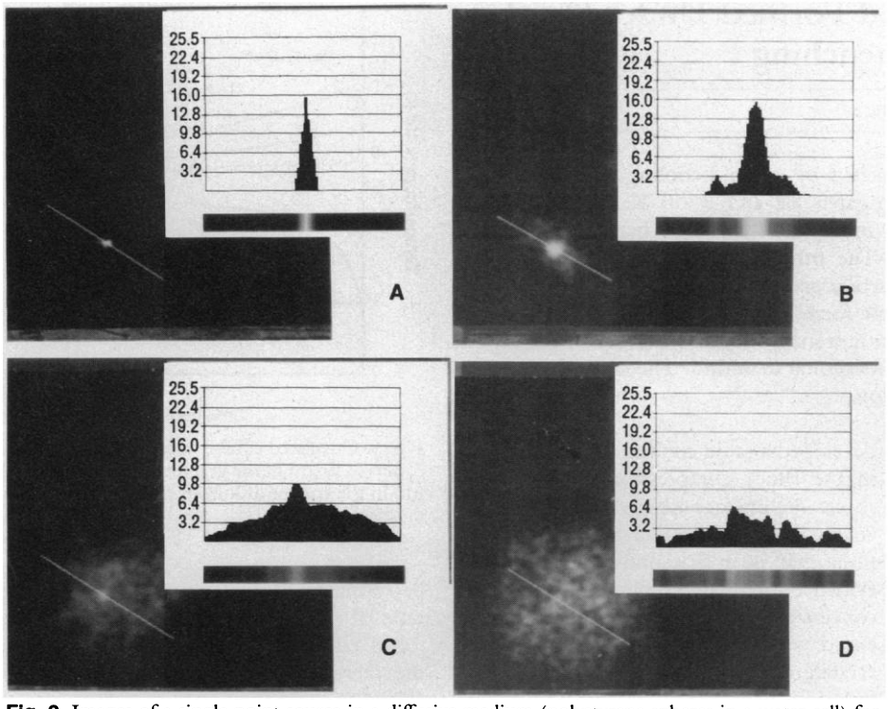

Fig. 2. Images of a single point source in a diffusive medium (polystyrene spheres in a water cell) for four different gating times: (**A**) $t = 0$; (**B**) $t = 10$ ps; (**C**) $t = 20$ ps; and (**D**) $t = 40$ ps. At $t = 0$, the ballistic light signal arrived and the image is sharp. At $t = 20$ ps, the scattering light starts to appear with a much larger radial intensity distribution in a forward-scattering solid angle around the point image. At $t = 40$ ps, the scattered light has spread out. No point image can be seen. Insets at the upper right corners are 1-D digitized intensity distributions as a function of distance through the white bar shown in the video photographs (left lower corner). The diameters of the digitized images (full width at half maximum) of these four photographs are (A) 200 μm, (B) 350 μm, (C) 900 μm, and (D) 1600 μm.

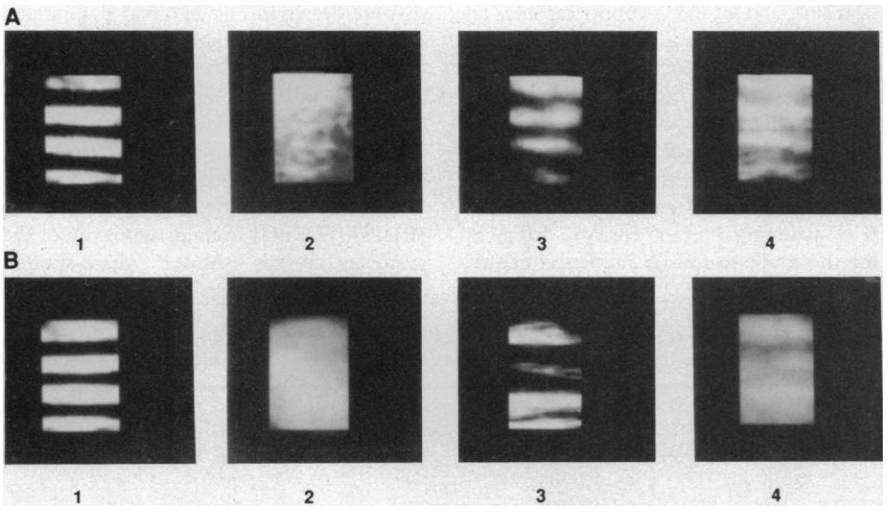

Fig. 3. Two-dimensional images of the test chart behind (**A**) 3.5-mm-thick human breast tissue and (**B**) 3-mm-thick chicken breast tissue illuminated by 8-ps, 530-nm laser pulses. The test object is a five line pairs per millimeter target from an Air Force bar test chart. Dark bars are the object, and the white area is the transparent background. The width of each bar is ~100 μm. (1) Reference image (tissue removed). (2) No time gate (standard transillumination). (3) $t_D = 0$, time gate at zero delay time. (4) $t_D = 22$ ps, time gate at 22-ps delay time. A 200-μm spatial resolution has been obtained in both photographs of (3) from the time-gated ballistic imaging. The image contrast is poor at a later delayed gate time as shown in (4). Without the time gate in (2), the image was totally blurred. Because of the high fiber content of chicken breast tissue, the resolution obtained from the time-gated ballistic imaging in (B3) is poorer than that from (A3). Part of the nonuniformity of the image at a time segment can be accounted for by the laser beam nonuniformity, the sample:refractive index variation, and internal structures.

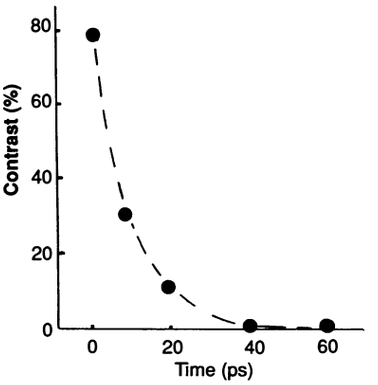

Fig. 4. Bar image contrast as a function of delayed gating time in turbid water. The measured contrast for the bar image in clear water was considered to be 100%. The horizontal axis is the delayed Kerr gate opening time in picoseconds.

time gate to increase the S/N ratio by an additional factor of 10^3. It is estimated that 2-D low-level signal images with an attenuation factor of e^{-30} through a scattering wall can be obtained. It is expected that it will soon be possible to detect highly resolved images of ultrasmall (less than a few millimeters) objects embedded inside thick biological and medical samples with the use of a high-repetition femtosecond multiple Kerr gate system.

REFERENCES AND NOTES

1. R. J. Coates *et al.*, *J. Natl. Cancer Inst.* **82**, 1684 (1990); G. S. Wilkson *et al.*, *J. Chron. Dis.* **32**, 365 (1979); N. Adam *et al.*, *J. Natl. Cancer Inst.* 76, 653 (1986).
2. NIH publication 88-2789 (1988).
3. B. Chance, Ed., *Photon Migration in Tissues* (Plenum, New York, 1990).
4. J. R. Singer, F. A. Grünbaum, P. Kohn, J. P. Zubelli, *Science* **248**, 990 (1990).
5. J. G. Fujimoto, S. De Dilversti, E. P. Ippen, R. Margolis, A. Oseroff, *Opt. Lett.* **11**, 150 (1986).
6. S. Andersson-Engels, R. Berg, S. Svanberg, O. Jarlman, *ibid.* **15**, 1179 (1990).
7. G. Navarro and A. Profio, *Med. Phys.* **15**, 181 (1988).
8. S. Webb, *The Physics of Medical Imaging* (IOP Publishing, New York, 1990).
9. R. Egan, *Breast Imaging* (Saunders, London, 1988).
10. J. C. Hebben and R. A. Kruger, *Med. Phys.* **17**, 351 (1990).
11. K. M. Yoo and R. R. Alfano, *Opt. Lett.* **15**, 320 (1990).
12. A. Ishimaru, *Wave Propagation and Scattering in Random Media* (Academic Press, New York, 1978).
13. M. A. Duguay and J. W. Hanson, *Appl. Opt.* **10**, 2162 (1971).
14. M. A. Duguay, *Am. Sci.* **59**, 550 (1971).
15. P. P. Ho and R. R. Alfano, *Phys. Rev. A* **17**, 2170 (1978).
16. S. L. Jacques, *Appl. Opt.* **28**, 2223 (1989).
17. R. Marchesini, A. Bertoni, E. Melloni, A. E. Sichirollo, *ibid.*, p. 2318; *Laser Surg. Med.* **8**, 142 (1988).
18. S. T. Flock, B. C. Wilson, M. S. Patterson, *Med. Phys.* **14**, 835 (1987).
19. P. P. Ho, R. Dorsinville, N. Yang, G. Eichmann, R. Alfano, *Proc. SPIE (Int. Soc. Opt. Eng.)* **682**, 36 (1986).
20. K. M. Yoo, Q. Xing, R. Alfano, *Opt. Lett.* **16**, 1091 (1991).
21. This research was supported in part by Hamamatsu Photonics K. K., Mediscience Technology Corp., and NIH.

18 April 1991; accepted 13 June 1991